Chapter 5
Exergetic Performance of the Desiccant Heating, Ventilating, and Air-Conditioning (DHVAC) System

Napoleon Enteria, Hiroshi Yoshino, Rie Takaki, Akashi Mochida, Akira Satake and Ryuichiro Yoshie

Abstract The developed desiccant heating, ventilating and air-conditioning (DHVAC) system was evaluated using the exergetic method under controlled environmental conditions to determine the performances of the whole system and its components. Percentage contributions of exergy destruction of system components at different regeneration temperatures and reference temperatures were determined. Exergy destruction coefficient of different components at different regeneration and reference temperatures was presented. It was shown that exergetic performances varied with respect to the regeneration and reference temperatures. The exergetic performances based on thermal, electric, total exergy input, first definition and second definition efficiencies were shown. Based on the results, reference and regeneration temperatures affected the determination of the system performances and its components. It was shown that air heating coil (AHC), air fans and desiccant wheel (DW) contributed to large percentage of exergy destruction. Hence, the mentioned components should be given attention for further improvement in the system performances.

Keywords Desiccant dehumidification · Evaporative cooling · Air handling system · Exergy analysis

This chapter is an updated version of our paper [1].

N. Enteria (✉)
Building Research Institute, Tsukuba, Japan
e-mail: napoleon@kenken.go.jp; enteria@enteria-ge.com

H. Yoshino · A. Mochida
Tohoku University, Sendai, Japan

R. Takaki
Akita Prefectural University, Akita, Japan

A. Satake
Maeda Corporation, Tokyo, Japan

R. Yoshie
Tokyo Polytechnic University, Atsugi, Japan

© Springer Nature Singapore Pte Ltd. 2017

N. Enteria et al. (eds.), *Desiccant Heating, Ventilating, and Air-Conditioning Systems*, DOI 10.1007/978-981-10-3047-5_5

Nomenclatures

AHC/HC	Air heating coil
C_p	Specific heat, kJ kg^{-1} K^{-1}
DEC/EC	Direct evaporative cooler
DHVAC	Desiccant heating, ventilating and air-conditioning
DW	Desiccant wheel
D_P	Depletion number
E	End
EA	Exit air
EAF	Exit air fan
HX [1]	Primary heat exchanger (big)
HX [2]	Secondary heat exchanger (small)
h	Enthalpy, kJ kg^{-1}
I_E	Electric current, A
I_{rr}	Irreversibility, kW
L, M, N	Variables
$\dot{m}$	Mass flow rate, kg s^{-1}
OA	Outdoor air
OAF	Outdoor air fan
P	Pressure, Pa
$\dot{Q}$	Heat transfer rate, kW
$\dot{Q}_X$	Input exergy in air heating coil, kW
R	Gas constant, kJ kg^{-1} K^{-1}
RA	Return air
RegT	Regeneration temperature
RT	Reference temperature
$\dot{S}$	Entropy rate, kW K^{-1}
S	Start
SA	Supply air
t	Time, s
T	Temperature, K
$\dot{W}$	Work rate, kW

Greek symbol

ε	Efficiency
ψ	Specific flow exergy, kJ kg^{-1}
ω	Humidity ratio, kg_{Vapor} kg_{Air}^{-1}
Φ	Relative humidity, %

Subscripts

a	Air
Des	Destruction
e	Exit
E_X	Exergy
Gen	Generation
HX	Heat exchanger
i	Inlet
l	Liquid
ma	Moist air
N	Node
o	Outlet
r	Reference condition
Sys	System
v	Vapor
w	Water

5.1 Introduction

Desiccant heating, ventilating and air-conditioning system (DHVAC) is one of the most promising alternatives to the refrigerant-based air-conditioning system [2, 3]. The main advantage of the desiccant-based air-conditioning system is the natural air dehumidification process called sorption process. The typical desiccant air-conditioning system consists of the desiccant wheel (DW), heat wheel and direct evaporative coolers (DECs) installed in the supply and return air (RA) streams [4–7]. Fixed bed [8, 9] and rotating desiccant dehumidifier [6, 10] are the most common desiccant dehumidifiers. However, rotating desiccant dehumidifier (desiccant wheel) is preferable for application due to its simplicity [2].

It is shown that determination of the exergetic performances of any thermal energy system gives more detailed and level playing field in the analysis of the system thermal performances [11]. In fact, there are several researches in the exergetic analyses on renewable energy systems [12, 13], thermal energy systems [14, 15], thermal system components [16], air handling systems [17–20] and buildings [21]. Exergetic analyses for the desiccant-evaporative air-conditioning system [22, 23], hybrid system [24, 25] and solar-desiccant air-conditioning system are studied [26].

In the exergetic evaluation of the desiccant air-conditioning system, it is shown that performances of the system components affected the system performance [27]. It is shown that higher regeneration temperature affected the system performance [28]. Shen and Worek [29] show that there is an optimal regeneration temperature in which the system performance is high. La et al. [23] show that there is trade-off

between the regeneration temperature and the exergy of the supply air (SA) that affects the system performance. This study presented the exergetic evaluation of the developed DHVAC system at different regeneration temperatures using steady-state conditions. The objective of the study is to determine the exergetic performances of the developed system and its components for further improvement also to evaluate the developed system performances in comparison with different desiccant-based air-conditioning systems.

5.2 Experimentation

5.2.1 System Overview

5.2.1.1 System Description

The system consists of the DW, sensible heat exchangers and a DEC. Figure 5.1 shows the developed DHVAC system diagram. In Fig. 5.1, the air from state 1 to state 3 is dehumidified by DW. The air from state 3 is pre-cooled by a sensible heat exchanger (HX [1]) and split into two streams of air (states 4 and 4′). The air from state 4′ is cooled by a DEC. The air of state 4 is sensibly cooled by smaller heat exchanger (HX [2]) from state 4 to state 5. The air at state 5 becomes the SA. The air at state 5 has the same humidity ratio as the processed air at state 3. The air at state 6 is mixed with the RA (state 7) for the preheating of hot air shown at state 9. The hot air at state 9 is heated by the air heating coil (AHC) to become the regeneration air (state 10). The regeneration air at state 10 is used to remove the

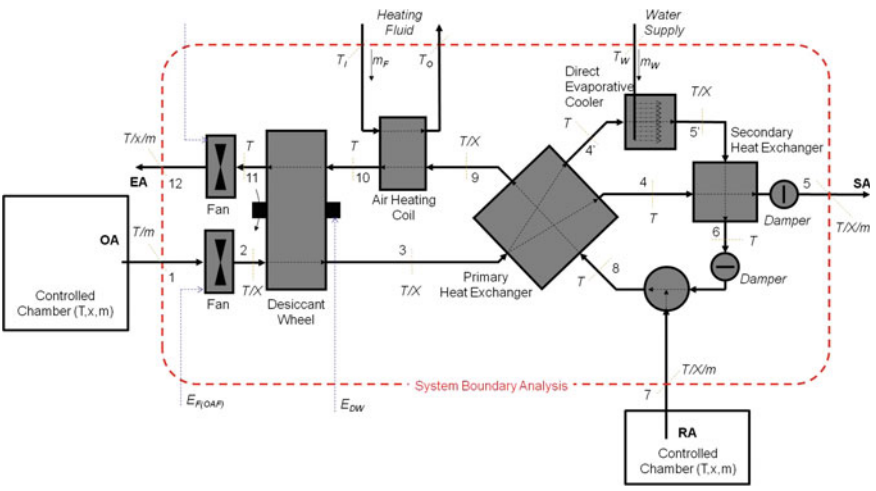

Fig. 5.1 Schematic diagram of the developed DHVAC system

moisture in the DW. The air at state 11 has higher humidity ratio due to regeneration process in the DW. The air at state 11 is exhausted by fan (EAF) to state 12.

5.2.1.2 Components Description

The system uses a honeycomb silica-gel-coated DW with 0.4 m diameter and 0.2 m thickness. The surface areas for air dehumidification side and wheel regeneration side are equal. The installed heat exchangers are cross-flow heat exchanges (sinusoidal flutes). The heat exchangers are made of paper coated with wax to avoid the transfer of moisture. The big heat exchanger (HX [1]) has dimensions of height 0.4 m, width 0.3 m and length 0.3 m. The smaller heat exchanger (HX [2]) has dimensions of height 0.4 m, width 0.15 m, and length 0.15 m. The DEC is a gravity flowing film type made of corrugated paper.

5.2.1.3 System Operation

The system operation is carried on using a controlled chamber (Chamber OA; See Fig. 5.1). The control of the RA conditions (T and x) is done by means of controlled chamber RA. The measurements of the air flow rates (outdoor air (OA), SA, RA and exit air) are determined by means of the orifices in the air duct with pressure difference sensors and temperature sensors. The control of air flow rates (OA, SA, RA and exit air) is done by the air dampers attached to the air ducts. The monitoring and control of the DW rotational speed are through the use of rotational laser sensor attached to the wheel belt. The control of the DEC is done by means of the relative humidity sensor attached at the downstream side (state 5′) through closed-loop control system. The control, monitoring and data gathering of the experimentation are made by means of the sensors attached to the experimental test rig of the desiccant-evaporative cooling system and connected to the personal computer through data logger.

5.2.2 Experimental Setup

5.2.2.1 Assembly

The total experimental setup has two controlled chambers (OA and RA) to control the condition of the air (temperature and humidity) as mentioned above (Sect. 5.2.1.3). Between the two controlled chambers, a working chamber in which the desiccant-evaporative cooling system is located with air ducts is connected (See Fig. 5.1). The air temperatures in the controlled chambers are controlled by the electric heater and air cooler using the heat pump. The heat pump serves also as the dehumidifier for the air, in case air dehumidification is needed. The humidification

process of the air is done through spray-type air humidifier. The operation of the two controlled chambers is meanly accomplished by passing the raw OA to the dehumidifier and cooler/heater device. In case low humidity is needed, dehumidification process operates. However, if the air becomes cool due to dehumidification process, electric heater operates to increase the temperature. In case when higher humidity of air is needed, the raw outside air passes the humidifier. The mixing chamber is installed after the air processing devices to control and homogenize the air prior to supplying it to the working chamber.

5.2.2.2 Instrumentations

All the attached sensors in the developed DHVAC system are evaluated and calibrated in the controlled box prior to their installation. The evaluated and calibrated sensors in the box are the dew point temperature sensors and the thermocouple temperature sensors. Based on the calibration, all the reading is within the specified value given by the manufacturers. Figure 5.1 shows the location and type of the sensors attached to the system. The measurement of the air humidity ratio is done by means of the dew point temperature sensors (±0.5 °C) and dry bulb temperature sensors (fabricated thermocouples). The fabricated thermocouples are from Japanese Industrial Standards (JIS) VT3, O 0.32 mm (±0.5 °C). Proper installations of dew point temperature and thermocouple probes are observed based on our previous experiences [30]. The measurement of the DW rotation is taken by the installed rotational laser sensor attached to the wheel belt. The measurement of air flow rates is taken using the installed orifices with digital pressure difference sensors (±3 Pa). The sensors attached to the DHVAC system are connected to the data logger. The data logger is then connected to the personal computer. In this measurement, the data gathering is made in every 30 s.

5.2.2.3 Cases

In the experimentation, the air conditions for the OA (Point 1) are set at value of 30 °C dry bulb temperature (2% accuracy) and 60% relative humidity (10% accuracy) (16.1 g kg^{-1}). This is the standard summer testing condition in Japan. The RA is set at value of 26 °C dry bulb temperature (1% accuracy) and 55% relative humidity (1% accuracy) (11.6 g kg^{-1}). This is the standard indoor air condition in Japan. The volumetric flow rates for the OA and exit air (EA) are set at 200 m^3 h^{-1}. The volumetric flow rates for the RA and SA are set 100 m^3 h^{-1}. The evaporative water inlet temperature is measured at 21.6 °C average and controlled by water heater to mimic the temperature of supply water pipe. The system is evaluated using the four different regeneration temperatures that can be supported by solar energy or low-temperature thermal energy source from waste heat. The

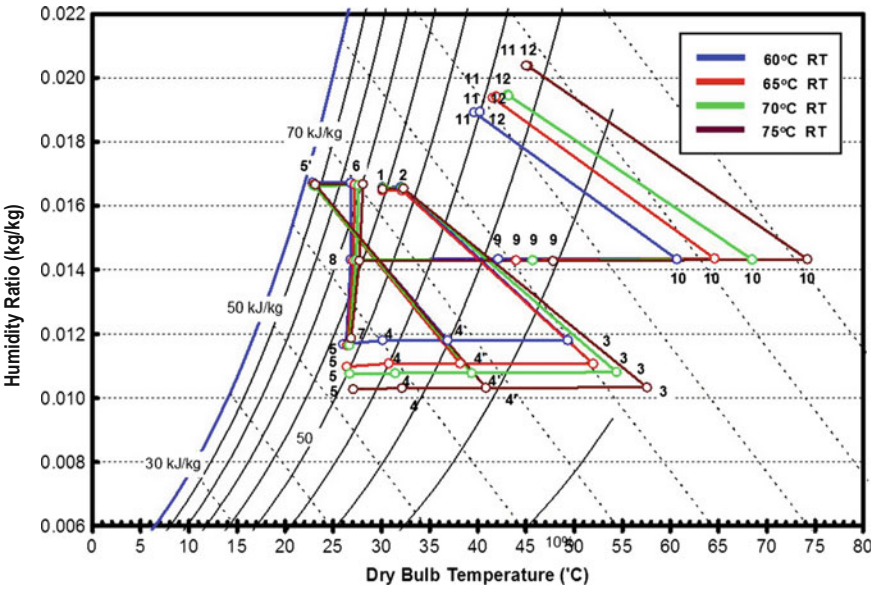

Fig. 5.2 States of air inside the developed DHVAC system in the psychrometric chart for different regeneration temperatures (RT)

Table 5.1 Measured air flow rates for different regeneration temperatures (RT) during the experimental evaluation of the developed DHVAC system

Regeneration temperature (°C)	OA		EA		SA		RA	
	$m^3\ h^{-1}$	$kg\ s^{-1}$	$m^3\ h^{-1}$	$kg\ s^{-1}$	$m^3\ h^{-1}$	$kg\ s^{-1}$	$m^3\ h^{-1}$	$kg\ s^{-1}$
60	201.18	0.0650	205.57	0.0646	94.31	0.0310	92.78	0.0306
65	201.32	0.0650	206.55	0.0646	94.30	0.0310	92.59	0.0305
70	200.65	0.0648	207.01	0.0645	94.27	0.0309	92.71	0.0305
75	200.33	0.0647	207.95	0.0645	94.38	0.0309	92.64	0.0305

regeneration temperatures used in the experimentation are 60, 65, 70 and 75 °C. Figure 5.2 shows the actual states of air inside the DHVAC system. Table 5.1 shows the measured air flow rates for the different regeneration temperatures presented in Fig. 5.2. Table 5.2 shows the values for the specific enthalpy, specific exergy and specific entropy for the different states inside the system for four cases of regeneration temperatures with reference states of 25 °C and 15 g kg^{-1}.

Table 5.2 Air states and equivalent specific enthalpy, specific entropy and specific exergy for different regeneration temperatures (RegT) for the case of 25 °C reference temperatures (RT)

State	Temperature, T (°C)				Humidity ratio, ω (g kg^{-1})				Specific enthalpy, h (kJ/kg)				Specific entropy, s (kJ/kg K)				Specific exergy, ψ (kJ/kg)			
	60 °C	65 °C	70 °C	75 °C	60 °C	65 °C	70 °C	75 °C	60 °C	65 °C	70 °C	75 °C	60 °C	65 °C	70 °C	75 °C	60 °C	65 °C	70 °C	75 °C
Reference	25				0.015				63.37				0.261				–			
1	30.1	30.1	30.2	30.1	0.0166	0.0165	0.0166	0.0165	72.7	72.5	72.7	72.6	0.296	0.295	0.296	0.295	0.056	0.055	0.057	0.055
2	32.0	32.1	32.2	32.3	0.0166	0.0165	0.0166	0.0165	74.7	74.5	74.8	74.8	0.302	0.302	0.303	0.303	0.096	0.097	0.100	0.101
3	49.3	52.0	54.4	57.6	0.0118	0.0111	0.0108	0.0103	80.2	81.1	82.8	84.8	0.306	0.306	0.310	0.315	1.026	1.269	1.498	1.826
4′	36.9	38.2	39.4	40.9	0.0118	0.0111	0.0108	0.0103	67.4	66.9	67.3	67.7	0.265	0.262	0.262	0.262	0.287	0.367	0.436	0.533
4	30.1	30.8	31.4	32.2	0.0118	0.0111	0.0108	0.0103	60.5	59.3	59.2	58.7	0.243	0.237	0.236	0.233	0.095	0.132	0.159	0.198
5′	22.9	22.9	23.0	23.1	0.0167	0.0167	0.0166	0.0167	65.5	65.5	65.5	65.7	0.272	0.272	0.272	0.273	0.021	0.020	0.019	0.018
5	26.0	26.4	26.7	27.1	0.0117	0.0110	0.0107	0.0103	56.0	54.6	54.3	53.5	0.227	0.221	0.219	0.215	0.055	0.083	0.095	0.120
6	26.8	27.2	27.6	28.1	0.0167	0.0167	0.0166	0.0167	69.6	69.9	70.3	70.8	0.286	0.287	0.288	0.290	0.018	0.021	0.024	0.029
7	26.3	26.4	26.7	26.9	0.0117	0.0116	0.0117	0.0119	56.3	56.3	56.6	57.3	0.228	0.228	0.229	0.232	0.056	0.058	0.059	0.053
8	26.8	27.1	27.4	27.7	0.0143	0.0143	0.0143	0.0143	63.5	63.6	64.1	64.3	0.259	0.260	0.261	0.262	0.008	0.010	0.012	0.015
9	42.1	44.0	45.7	47.8	0.0143	0.0143	0.0143	0.0143	79.3	81.1	83.0	85.1	0.311	0.316	0.322	0.329	0.496	0.606	0.716	0.869
10	60.7	64.6	68.5	74.2	0.0143	0.0143	0.0143	0.0143	98.4	102.3	106.5	112.3	0.370	0.381	0.394	0.410	2.060	2.518	3.016	3.823
11	39.6	41.5	43.1	45.2	0.0189	0.0194	0.0194	0.0204	88.6	91.8	93.6	98.2	0.354	0.365	0.371	0.388	0.429	0.545	0.637	0.808
12	40.2	41.9	43.2	45.4	0.0189	0.0194	0.0194	0.0204	89.2	92.2	93.7	98.4	0.356	0.367	0.371	0.389	0.458	0.563	0.643	0.819
Water	21.6	21.7	21.6	21.7	–	–	–	–	90.7	90.8	90.3	90.7	0.319	0.320	0.318	0.320	0.080	0.078	0.083	0.079

5.3 Thermodynamic Analysis

5.3.1 General Formulation

The evaluation of the DHVAC system is based on the governing concept of the laws of thermodynamics. The general formulations for exergy analyses of the thermal system are presented in Eqs. (5.1–5.12) and applied in the DHVAC system of thermodynamic model shown in Fig. 5.1. In these formulations, the reference states are the T_r, Φ_r, ω_r, P_r.

The general mass rate balance for the open system is

$$\sum_{j=1}^{N} \dot{m}_{j,I} - \sum_{i=1}^{M} \dot{m}_{i,O} = \frac{\mathrm{d}m_{\mathrm{Sys}}}{\mathrm{d}t} \tag{5.1}$$

The general energy rate balance for the open system is

$$\sum_{j=1}^{N} \dot{Q}_{j,I} + \sum_{i=1}^{N} \left(\dot{m}_j h_j\right)_I = \sum_{i=1}^{M} \dot{W}_{i,O} + \sum_{i=1}^{M} \left(\dot{m}_i h_i\right)_O \tag{5.2}$$

The general exergy rate balance for the open system is

$$\sum_{j=1}^{N} \left[1 - \left(\frac{T_r}{T_{K,j}}\right)\right] \dot{Q}_{K,j} + \sum_{j=1}^{N} \left(\dot{m}_j \psi_j\right)_I = \sum_{i=1}^{M} \dot{W}_{i,O} - \sum_{i=1}^{M} \left(\dot{m}_i \psi_i\right)_O \tag{5.3}$$

The general entropy generation rate for the open system is

$$\dot{S}_{\mathrm{Gen}} = \sum_{i=1}^{N} \left(\dot{m}_i s_i\right)_O - \sum_{j=1}^{M} \left(\dot{m}_j s_j\right)_I - \sum_{k=1}^{L} \left(\frac{Q_{S,k}}{T_{S,k}}\right) \tag{5.4}$$

The general exergy rate of destruction or the rate of irreversibility is

$$\dot{E}_{X,\mathrm{Dest}} = I_{\mathrm{rr}} = T_r \dot{S}_{\mathrm{Gen}} = \sum_{j=1}^{N} \left(\dot{E}_{x,j}\right)_I - \sum_{i=1}^{M} \left(\dot{E}_{x,i}\right)_O \tag{5.5}$$

The general exergetic efficiency for the open system is

$$\varepsilon_X = \frac{\left[\sum_{i=1}^{M} \dot{W}_{i,O} + \sum_{i=1}^{M} \left(\dot{m}_i \psi_i\right)_O\right]}{\left\langle \sum_{j=1}^{N} \left[1 - \left(\frac{T_r}{T_{K,j}}\right)\right] \dot{Q}_{K,j} + \sum_{j=1}^{N} \left(\dot{m}_j \psi_j\right)_I \right\rangle} = \frac{\sum_{i=1}^{M} \left(\dot{E}_{x,i}\right)_O}{\sum_{j=1}^{N} \left(\dot{E}_{x,j}\right)_I} \tag{5.6}$$

The relative destruction (RD) of exergy for the open system is presented as

$$\mathrm{RD} = \frac{\left(\dot{E}_{X,\mathrm{Dest}}\right)_t}{\sum_{t=1}^{C} \dot{E}_{X,\mathrm{Dest}}} \cdot 100 \tag{5.7}$$

The Van Gool's improvement potential (IP) for the open system is presented as [12]

$$\mathrm{IP} = (1 - \varepsilon_X) \cdot \left(\sum_{j=1}^{N} \left(\dot{E}_{x,j}\right)_I - \sum_{i=1}^{M} \left(\dot{E}_{x,i}\right)_O \right) \tag{5.8}$$

The Van Gool's IP is the maximum possible IP that could be done for any processes through minimization of the exergy destruction or the difference between the inlet exergy and outlet exergy.

The sustainability index (SI) for the open system can be expressed as [31]

$$\mathrm{SI} = \frac{\sum_{j=1}^{N} \left(\dot{E}_{x,j}\right)_I}{\sum_{j=1}^{N} \left(\dot{E}_{x,j}\right)_I - \sum_{i=1}^{M} \left(\dot{E}_{x,i}\right)_O} = \frac{1}{1 - \varepsilon_X} = \frac{1}{D_P} = \frac{\sum_{j=1}^{N} \left(\dot{E}_{x,j}\right)_I}{\sum_{t=1}^{C} \dot{E}_{X,Dest}} \tag{5.9}$$

The SI is an inverse of the depletion number (D_p), which is the relationship between the exergy destruction of the exergy input. When the exergy destruction decreases even with the same exergy input due to the increase in the efficiency, the SI increases. It means that less fuel is consumed particularly when using conventional sources.

The specific flow exergy is

$$\psi = (h - h_\mathrm{r}) - T_\mathrm{r}(s - s_\mathrm{r}) \tag{5.10}$$

The specific exergy of incompressible substance such as water is [19]

$$\psi_\mathrm{w} = C_{\mathrm{P,w}}(T_\mathrm{w} - T_\mathrm{r}) - T_\mathrm{r} C_{\mathrm{P,w}} \ln\left(\frac{T_\mathrm{w}}{T_\mathrm{r}}\right) - R_\mathrm{v} T_\mathrm{r} \ln \varphi_\mathrm{r} \tag{5.11}$$

φ_r is the equivalent relative humidity at reference temperature (T_r) and humidity ratio (ω_r). The specific exergy of moist air is [12]

$$\begin{aligned}\psi_\mathrm{ma} = {} & \left\langle (C_{\mathrm{p,g}} + \omega C_{\mathrm{p,v}}) T_\mathrm{r} \left[\left(\frac{T_\mathrm{ma}}{T_\mathrm{r}}\right) - 1 - \ln\left(\frac{T_\mathrm{ma}}{T_\mathrm{r}}\right) \right] \right\rangle + \left[(1 + 1.607\omega) T_\mathrm{r} \ln\left(\frac{P_\mathrm{ma}}{P_\mathrm{r}}\right) \right] \\ & + R_\mathrm{g} T_\mathrm{r} \left\langle (1 + 1.607\omega) \ln\left[\frac{(1 + 1.607 w_\mathrm{r})}{(1 + 1.7607\omega)}\right] + 1.607 \ln\left(\frac{\omega}{\omega_\mathrm{r}}\right) \right\rangle \end{aligned} \tag{5.12}$$

5.3.2 System Analysis

5.3.2.1 Desiccant Wheel (DW) Exergy Efficiency

$$(\varepsilon_X)_{\mathrm{DW}} = \frac{[\dot{m}_{\mathrm{OA}}(\psi_3 - \psi_2)]}{\left\langle \left(\dot{E}_E\right)_{\mathrm{DW}} + [\dot{m}_{\mathrm{EA}}(\psi_{10} - \psi_{11})] \right\rangle} \tag{5.13}$$

5.3.2.2 Sensible Heat Exchanger (HX [1]/HX [2]) Exergy Efficiency

$$(\varepsilon_X)_{\mathrm{HX}(1)} = \frac{[\dot{m}_{\mathrm{EA}}(\psi_9 - \psi_8)]}{\left\langle \dot{m}_{\mathrm{OA}} \left\{ \psi_3 - \left[\frac{(\psi_{4'} + \psi_4)}{2} \right] \right\} \right\rangle} \tag{5.14}$$

$$(\varepsilon_X)_{\mathrm{HX}(2)} = \frac{[(\dot{m}_{\mathrm{OA}} - \dot{m}_{\mathrm{SA}})(\psi_6 - \psi_{5'})]}{[\dot{m}_{\mathrm{SA}}(\psi_4 - \psi_5)]} \tag{5.15}$$

5.3.2.3 Direct Evaporative Cooler (DEC) Exergy Efficiency

$$(\varepsilon_X)_{\mathrm{EC}} = \frac{[(\dot{m}_{\mathrm{OA}} - \dot{m}_{\mathrm{SA}})\psi_{5'}]}{\langle [\dot{m}_{\mathrm{W}}\psi_{\mathrm{W}}] + [(\dot{m}_{\mathrm{OA}} - \dot{m}_{\mathrm{SA}})\psi_{4'}] \rangle} \tag{5.16}$$

5.3.2.4 Air Heating Coil (AHC) Exergy Efficiency

$$(\varepsilon_X)_{\mathrm{AH}} = \frac{[\dot{m}_{\mathrm{EA}}(\psi_{10} - \psi_9)]}{[\dot{m}_{\mathrm{L}}(\psi_{\mathrm{T}} - \psi_{\mathrm{S}})]} \tag{5.17}$$

5.3.2.5 Air Fan (OAF and EAF) Exergy Efficiency

$$(\varepsilon_X)_{F(\mathrm{OAF})} = \frac{\left[\dot{m}_{F(\mathrm{OAF})}(\psi_2 - \psi_1)\right]}{\left(\dot{E}_E\right)_{F(\mathrm{OAF})}} \tag{5.18}$$

$$(\varepsilon_X)_{F(\mathrm{EAF})} = \frac{\left[\dot{m}_{F(\mathrm{EAF})}(\psi_{12} - \psi_{11})\right]}{\left(\dot{E}_E\right)_{F(\mathrm{EAF})}} \tag{5.19}$$

5.3.2.6 System Exergetic Performances

Electric exergetic coefficient of performance (EE_XCOP):

$$\left[(\varepsilon_X)_{\mathrm{Sys}}\right]_{\mathrm{Electric}} = \frac{[\dot{m}_{\mathrm{SA}}(\psi_1 - \psi_5)]}{\left\langle \left(\dot{E}_{\mathrm{E}}\right)_{\mathrm{DW}} + \left(\dot{E}_{\mathrm{E}}\right)_{F(\mathrm{OAF})} + \left(\dot{E}_{\mathrm{E}}\right)_{F(\mathrm{EAF})} \right\rangle} \tag{5.20}$$

Thermal exergetic coefficient of performance (TE_XCOP):

$$\left[(\varepsilon_X)_{\mathrm{Sys}}\right]_{\mathrm{Thermal}} = \frac{[\dot{m}_{\mathrm{SA}}(\psi_1 - \psi_5)]}{\dot{Q}_X} \tag{5.21}$$

Total exergetic coefficient of performance (SE_XCOP):

$$\left[(\varepsilon_X)_{\mathrm{Sys}}\right]_{\mathrm{Total}} = \frac{[\dot{m}_{\mathrm{SA}}(\psi_1 - \psi_5)]}{\left\langle \dot{Q}_X + \left(\dot{E}_E\right)_{\mathrm{DW}} + \left(\dot{E}_E\right)_{F(\mathrm{OAF})} + \left(\dot{E}\right)_{F(\mathrm{EAF})} + (\dot{m}_{\mathrm{W}}\psi_{\mathrm{W}}) \right\rangle} \tag{5.22}$$

The calculation of thermal exergy delivered to the air heating coil (HC) is based on

$$\dot{Q}_X = \dot{m}_F C_{\mathrm{p}} \left[(T_I - T_O) - T_{\mathrm{r}} \ln\left(\frac{T_I}{T_O}\right) \right] \tag{5.23}$$

5.3.2.7 System Exergetic Efficiencies

The actual thermal coefficient of performance is simply the ratio of the cooling produced to the thermal energy supplied as

$$\mathrm{COP_A} = \frac{\dot{m}_{\mathrm{SA}}(h_1 - h_5)}{\dot{m}_{\mathrm{EA}}(h_{10} - h_9)} \tag{5.24}$$

The Carnot coefficient of performance for any heat-driven air-conditioning system is shown based on the diagram shown in Fig. 5.1.

$$\mathrm{COP_C} = \left(1 - \frac{T_1}{T_{10}}\right)\left(\frac{T_7}{T_1 - T_7}\right) \tag{5.25}$$

The $\mathrm{COP_C}$ is the highest potential of the coefficient of performance for any heat-driven air-conditioning system, which is mostly applied in closed cycles.

The proposed reversible Carnot coefficient of performance for the open-cycle desiccant air-conditioning system is expressed as [27]

$$\mathrm{COP_{Rev}} = \left(1 - \frac{T_c}{T_s}\right)\left(\frac{T_e}{T_c - T_e}\right) \tag{5.26}$$

where T_s, T_e and T_c are equivalent temperatures for the heat source, evaporator and condenser and are expressed based on Fig. 5.1

$$T_s = \frac{h_9 - h_{10}}{s_9 - s_{10}} \tag{5.27}$$

$$T_e = \frac{\dot{m}_{SA}h_5 - \dot{m}_{RA}h_7 + \dot{m}_{W(5\to7)}h_w}{\dot{m}_{SA}s_5 - \dot{m}_{RA}s_7 + \dot{m}_{W(5\to7)}s_w} \tag{5.28}$$

$$T_c = \frac{\dot{m}_{OA}h_1 - \dot{m}_{EA}h_{12} - \left(\dot{m}_{w(5\to7)} + m_{w(4'\to5')}\right)h_w}{\dot{m}_{OA}s_1 - \dot{m}_{EA}s_{12} - \left(\dot{m}_{w(5\to7)} + m_{w(4'\to5')}\right)s_w} \tag{5.29}$$

The exergy efficiency can be expressed as the ratio of the actual coefficient of performance for the thermal-driven air-conditioning system to the reversible coefficient of performance [32]. It is called as the exergy efficiency in the first definition here.

$$(\varepsilon_X)_1 = \frac{\mathrm{COP_A}}{\mathrm{COP_{Rev}}} \tag{5.30}$$

For comparison purposes with different studies in thermal-driven air-conditioning systems, the exergy efficiency is expressed based on the ratio of the cooling produced to the thermal exergy supplied as (exergy efficiency in the second definition) [32].

$$(\varepsilon_X)_2 = \frac{\dot{m}_{SA}(\psi_1 - \psi_5)}{\dot{m}_{EA}(\psi_{10} - \psi_9)} \tag{5.31}$$

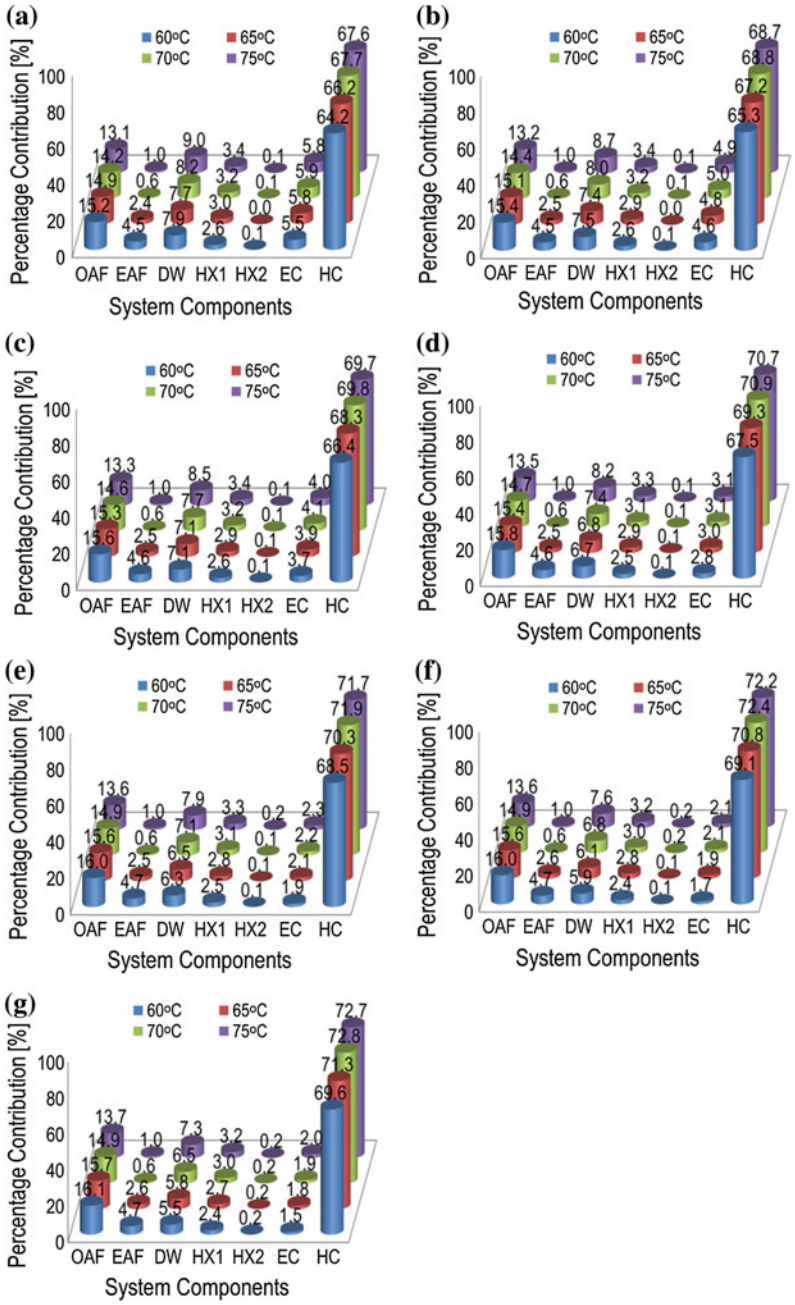

Fig. 5.3 Percentage contribution of exergy destruction for the developed DHVAC system components at different regeneration temperatures (RegT) and reference temperatures (RT): **a** 0 °C RT; **b** 5 °C RT; **c** 10 °C RT; **d** 15 °C RT; **e** 20 °C RT; **f** 25 °C RT, and; **g** 30 °C RT

5.4 Results and Discussion

5.4.1 Exergy Destruction Contribution

Figure 5.3 shows the exergy destruction contribution of the developed DHVAC system at different regeneration temperatures and reference temperatures. The air heating coil (AHC) is contributed to high percentage of the total exergy destruction: the same trend for exergy destruction for the case of Hurdogan et al. [25], which shows that system thermal source and air fans are the main contributors. The destruction contribution is followed by the outdoor air fan (OAF) and then by the DW. As the regeneration temperature increases, the contribution of the AHC to exergy destruction increases. Kodama et al. [28] show that heat source and DW are major sources of exergy destruction (air fans are not considered in their analysis). The exergy destruction contribution of the DW increases as the regeneration temperature increases. The trend for the exergy destruction contributions for the heat exchangers (HX1 and HX2) and direct evaporative cooler (EC) increases as the regeneration temperature increases due to the increase in the components irreversibility. Furthermore, based on the different reference temperatures, it shows the increase in the AHC exergy destruction contribution.

5.4.2 Exergy Destruction Coefficient

Figure 5.4 shows the exergy destruction coefficient for different components of the developed DHVAC system at different regeneration temperatures and reference temperatures. The trend of the exergy destruction coefficient is the same as the exergy destruction contribution presented in Fig. 5.3. The HC has the largest exergy destruction coefficient followed by the OAF and DW. The exergy destruction in the AHC could be lowered by increasing the efficiency of the AHC. La et al. [23] show also that heat source has the largest exergy destruction coefficient. It also shows that when the regeneration temperature increases, the exergy destruction coefficient for the AHC increases due to the increase in heat transfer irreversibility. It is the same for the cases of DW and heat exchangers (HX1 and HX2) and evaporative cooler (EC). On the other hand, when the reference temperature increases, the exergy destruction coefficient for HC increases.

5.4.3 System Performances

Figure 5.5a shows the thermal exergetic coefficient of performance of the system. The thermal exergetic coefficient of performance (TE_XCOP) is varied with the reference temperature, and from 0 to 22 °C, the thermal exergetic performance of

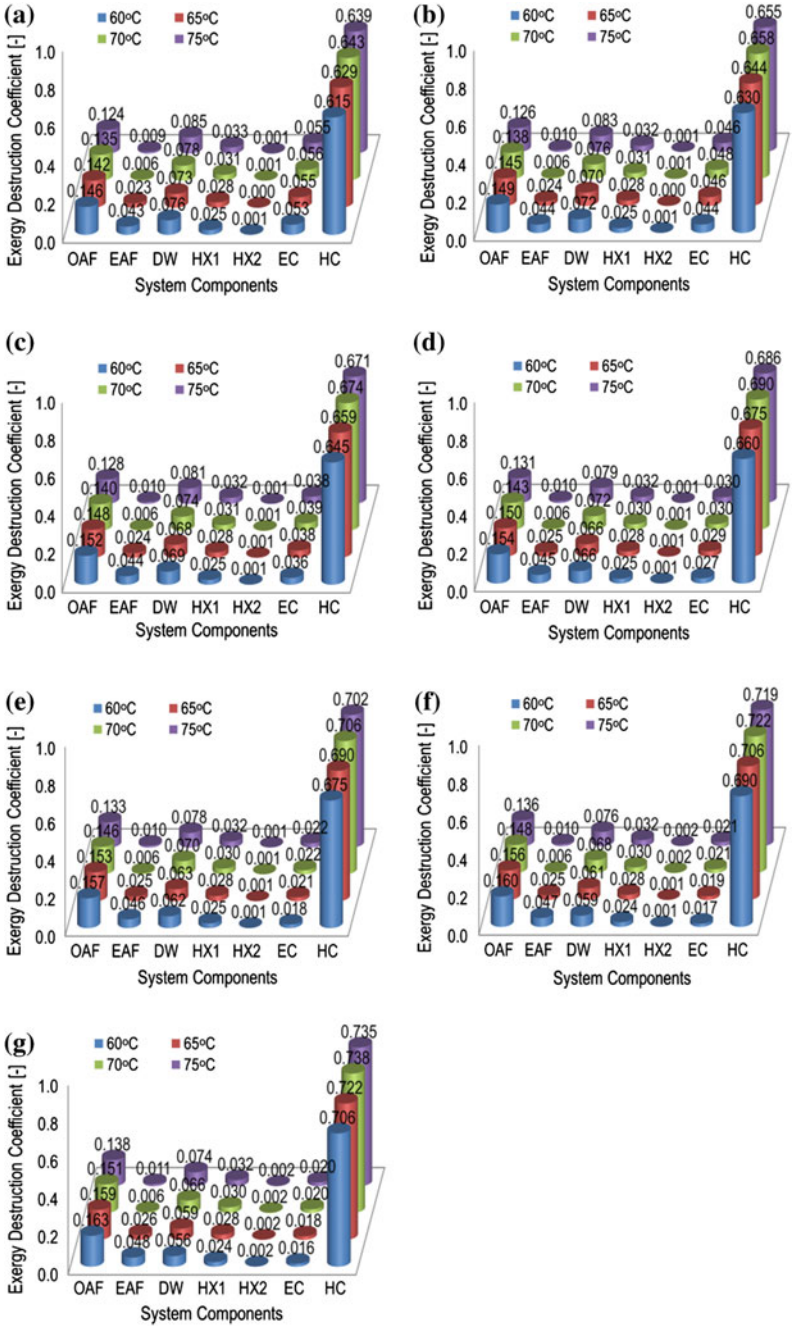

Fig. 5.4 Exergy destruction coefficient for the developed DHVAC system components at different regeneration temperatures (RegT) and reference temperatures (RT): **a** 0 °C RT; **b** 5 °C RT; **c** 10 °C RT; **d** 15 °C RT; **e** 20 °C RT; **f** 25 °C RT, and; **g** 30 °C RT

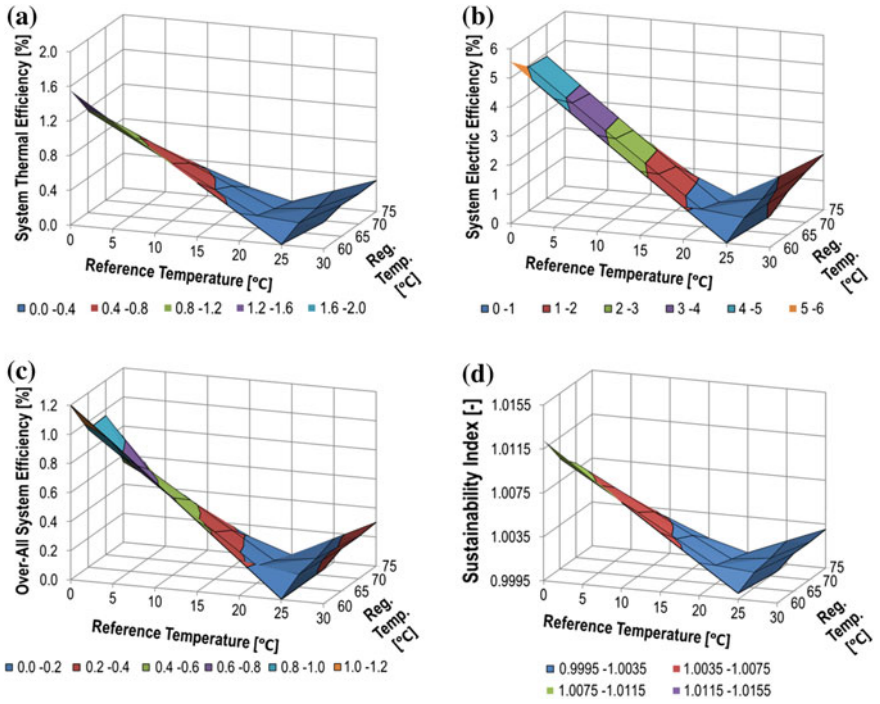

Fig. 5.5 Performances of the developed DHVAC system at different regeneration temperatures (RegT) and reference temperatures (RT): **a** thermal exergetic COP with respect to different reference temperatures (RT) and regeneration temperatures (RegT); **b** electric exergetic COP with respect to different reference temperatures (RT) and regeneration temperatures (RegT); **c** system exergetic COP with respect to different reference temperatures (RT) and regeneration temperatures (RegT); and **d** sustainability index with respect to different reference temperatures (RT) and regeneration temperatures (RegT)

the system decreases, after which the performance increases. However, based on the different regeneration temperatures, from 0 to 22 °C, the thermal exergetic performance of the system decreases as the regeneration temperature increases and suddenly changed from 22 to 30 °C. On the other hand, for the electric exergetic performance presented in Fig. 5.5b, the trend of the electric exergetic coefficient of performance (EE_XCOP) is the same as the thermal exergetic coefficient of performance shown in Fig. 5.5a in terms of reference temperatures. It means that increasing the regeneration temperature also affects the electric consumption of the system due to the increase in system internal frictional losses which resulted in the decrease in the EE_XCOP. On the other hand, the increase in the regeneration temperature results in higher increase in the system thermal exergy destruction due to components irreversibility and results in the decrease in the TE_XCOP as

explained in the different components. Figure 5.5c shows the overall system exergetic coefficient of performance (SE_XCOP). It shows the same trend based on regeneration temperature and reference temperatures. Based on the analysis of each of the three exergetic coefficient of performances (TE_XCOP, EE_XCOP and SE_XCOP), the system performance decreases as the regeneration temperature increases. Furthermore, there is a sudden decrease in the performance from 60 to 65 °C and 70 to 75 °C. Based on Fig. 5.2, the dehumidification and cooling of SA (Point 5) are almost the same for regeneration temperatures of 65 and 70 °C. The SI shows that as the regeneration temperature increases, the SI decreases from 0 to 22 °C and changed from 22 to 30 °C (Fig. 5.5d). The SI is related to exergy efficiency as shown in Eq. (5.9). Hence, from Fig. 5.5c, the overall system exergy efficiency varies as the dead state temperature changes. This is the same trend for the case of the evaporative cooler shown by Caliskan et al. [33].

Figure 5.6a shows the reversible coefficient of performance (COP_{Rev}). It shows that the COP_{Rev} has nothing to do with the reference temperature. As presented, the COP_{Rev} suddenly increases from 60 °C regeneration temperature to 65 °C. The COP_{Rev} then reduces at 70 °C and increases a little at 75 °C. This trend of COP_{Rev} is due to the system dehumidification performance shown in Fig. 5.2. As shown in Fig. 5.2, there is a large increase in the system dehumidification performance from 60 to 65 °C, which resulted in higher increase in COP_{Rev}, and then from 65 to 70 °C, the dehumidification performance is not large even with this same increase in regeneration temperature of 5 °C. In addition, from 70 to 75 °C, the increase is not as large as from 60 to 65 °C; this resulted in lower increase in $COP_{Rev.}$ This trend has little increase in the dehumidification performance of the DW, resulting from the heating of the desiccant material in the dehumidification side due to the heat carry over from the regeneration side to dehumidification side of the DW as observed from our previous studies [30]. The present system has higher COP_{Rev} of 4.20 at regeneration temperature of 65 °C. Lavan et al. [27] got 4.66, while Kanoglu et al. [34] got a COP_{Rev} of 2.63 for double wheel + double evaporative coolers of DHVAC system.

Figure 5.6b shows that the actual coefficient of performance (COP_A) is higher at regeneration temperature of 60 °C and suddenly decreases as the regeneration increases to 75 °C. This trend of decreasing COP_A as the regeneration temperature increases is due to the non-proportional increase in the system cooling capability as the regeneration energy supported to the system increases as the regeneration temperature increases. As the regeneration temperature increases, the heat carry over from the regeneration side of the DW to its dehumidification side increases [30]. The increase in the DW temperature in the dehumidification side hampered the adsorption capacity as the sorption process is the difference of the water vapor pressure between the air and the desiccant surface. Also, the increase in the regeneration temperature increases the exergy of the SA. As shown in Fig. 5.2, the increase in the air temperature after the DW (state 3) is almost linear compared to the increase in the dehumidification capability as the regeneration temperature increases. Kodama et al. [28] show the same trend of result.

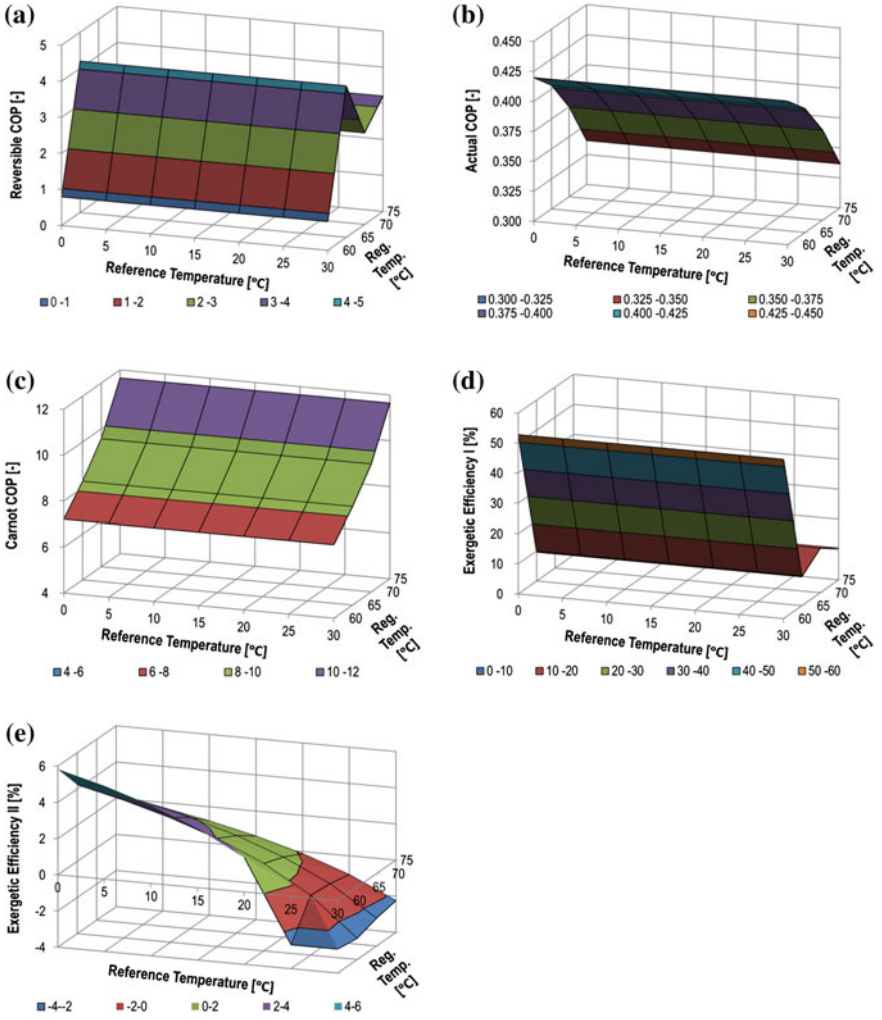

Fig. 5.6 Performances of the developed DHVAC system at different regeneration temperatures (RegT) and reference temperatures (RT): **a** reversible Carnot coefficient of performance $(COP)_{Rev}$ with respect to different reference temperatures (RT) and regeneration temperatures (RegT); **b** actual coefficient of performance $(COP)_{Act}$ with respect to different reference temperatures (RT) and regeneration temperatures (RegT); **c** Carnot coefficient of performance $(COP)_C$ with respect to different reference temperatures (RT) and regeneration temperatures (RegT); **d** Exergetic efficiency I (First Definition); and **e** Exergetic efficiency II (second definition)

Figure 5.6c shows the Carnot coefficient of performance (COP_C), which presents the increasing trend as the regeneration temperature increases. The increasing trend of the COP_C is due to the increase in the regeneration temperature (T_{10}). In addition, as shown in this research, the return temperature (T_7) and the outdoor temperature

(T_7) are held constant. These values of the COP_C are the possible Carnot coefficient of performance of the heat-driven cooling system at closed-cycle equivalent. However, open-cycle DHVAC system is not only for the temperature control but also for the humidity control. Therefore, the actual and the reversible coefficients of performances (COP_A and COP_{Rev}) are different as explained in the above discussions for the COP_A and COP_{Rev}. For comparison purposes, Kanoglu et al. [34] presented a COP_C of 8.74 based on ARI conditions. In this paper, the COP_C at 75 °C is 11.65.

Figure 5.6d shows the exergetic efficiency of first definition (exergetic efficiency I), which shows the decreasing trend as the regeneration temperature increases. The lowest value can be seen in the regeneration temperature of 70 °C, which has also a lower value of $COP_{Rev.}$ It shows that at 60 °C, the exergetic efficiency I is 52.77%, while the lowest is 9.61% at 60 °C. Figure 5.6e shows the decreasing trend of the exergetic efficiency of the second definition (exergetic efficiency II). The negative value of the second definition is due to the increase in the SA exergy upon increase in the reference temperature. The exergetic efficiency of second definition decreases as the regeneration temperature increases due to the smaller increase in the cooling exergy capability of the system even with the increasing regeneration exergy supply to the system. This explanation is the same to the actual coefficient of performance (COP_A). Moreover, the exergetic coefficient of performance of second definition decreases as the reference temperature increases. It means that at higher temperature, the system exergetic performance of second definition is not as efficient as in lower reference temperature due to the reduction in the system cooling exergy produced. Hence, it is expensive and inefficient to operate the system at higher OA temperature than at lower OA temperature.

5.5 Conclusions

This paper showed the exergy evaluation of the developed DHVAC system. The developed system was evaluated based on different regeneration temperatures and reference temperatures in which the system will be subjected to its actual operation.

- AHC, OAF and then DW contributed to high percentage of the total exergy destruction.
- Based on the analysis of each of the three exergetic coefficient of performances (TE_XCOP, EE_XCOP and SE_XCOP), the system performance decreases as the regeneration temperature increases.
- The SI shows that as the regeneration temperature increases, the SI decreases from 0 to 22 °C and changed from 22 to 30 °C (Fig. 5.5d).
- The COP_{Rev} suddenly increases from 60 °C regeneration temperature to 65 °C. The COP_{Rev} then reduces at 70 °C and then increases a little at 75 °C. The trend of COP_{Rev} is due to the system dehumidification performance shown in Fig. 5.2.

- The actual coefficient of performance (COP_A) is higher at regeneration temperature of 60 °C and decreases as the regeneration temperature increases to 75 °C. This trend of decreasing COP_A as the regeneration temperature increases is due to the not proportional increase in the system cooling capability as the regeneration energy supported to the system increases as the regeneration temperature increases.
- The increasing trend of the COP_C as the regeneration temperature increases is due to the increase in the regeneration temperature (T_{10}). In addition, as shown in this research, the return temperature (T_7) and the outdoor temperature (T_7) are held constant.
- The exergetic efficiency of first definition (exergetic efficiency I) shows the decreasing trend as the regeneration temperature increases. The lowest value can be seen in the regeneration temperature of 70 °C, which has also a lower value of $COP_{Rev.}$
- The exergetic efficiency of second definition decreases as the regeneration temperature increases due to the little increase in the cooling exergy capability of the system even with the increasing regeneration exergy supply to the system.

The exergetic evaluation is valuable in the evaluation of the DHVAC system we developed. It shows which components with large destruction of exergy that resulted in lowering of the system exergy efficiencies. AHC, air fans (OAF and EAF) and DW contributed to large percentage of system exergy destruction, resulting in large impact of the reduction in the system performance. Hence, it is important to consider the components with high exergy destruction such as the AHC, air fans and DW for improvement.

It was shown that the system presented in this paper which has one evaporative cooler and two sensible heat exchangers could have better performance compared to the typical double wheels and double evaporative coolers. For comparison purposes, the exergetic efficiency of the liquid DHVAC system is still high (6.8%, the lowest, for the basic system) [34, 35]; however, handling of the liquid desiccant is more complex than solid desiccant. In the case of the solid desiccant, multi-staging will increase the exergetic efficiency from 8.2 to 18.0% [22, 23]. However, multi-staging and making the air flow complex increase the fan power consumption that will affect the system performance when fan exergy input is considered for our case. With respect to the closed-cycle water–LiBr desiccant system, the open system has comparable COP_A at lower regeneration temperature to half-effect and single-effect water–LiBr desiccant system shown by Gebreslassie et al. [36] and Kaushik and Arora [37]. For example, in this paper, the COP_A is 0.42 at 60 °C, while the water–LiBr desiccant system of half effect has 0.458 [36]. However, when converting the closed-cycle water–LiBr system to cool and dehumidify the air, it is expected that the COP_A will be lower. With respect to the closed-cycle, solid desiccant system, the COP_A is lower but could operate at much lower regeneration temperature. For example, at 60 °C temperature, it could have a COP of less than 0.2 [38], which is less than the open-cycle counterpart. Askalany et al. [39] presented some pairs of solid desiccant and refrigerant, which could have higher COP. Hence, application of different types of desiccant-based air-conditioning system depends on the need and specific target. Wang et al. [40] presented important guidelines

of the desiccant-based air-conditioning system. For the case of open-cycle DHVAC system, it offers some advantages for chemical and biological treatments of the SA to the indoor environment [2]. Further investigation through exergoeconomic and exergoenvironmental analyses had been done to deepen the evaluation of the developed DHVAC system [41, 42].

References

1. Enteria N, Yoshino H, Takaki R et al (2013) Effect of regeneration temperatures in the exergetic performances of the developed desiccant-evaporative air-conditioning system. Int J Refrig 36:2323–2342
2. Enteria N, Mizutani K (2011) The role of the thermally activated desiccant cooling technologies in the issue of energy and environment. Renew Sust Energ Rev 15:2095–2122
3. Choudhury B, Saha BB, Chatterjee PK et al (2013) An overview of developments in adsorption refrigeration systems towards a sustainable way of cooling. Appl Energ 104: 554–567
4. Henning HM, Erpenbeck T, Hindenburg C et al (2001) The potential of solar energy use in desiccant cooling cycles. Int J Refrig 24:220–229
5. Panaras G, Mathioulakis E, Belessiotis V (2011) Solid desiccant air-conditioning systems—design parameters. Energy 36:2399–2406
6. Hurdogan E, Buyukalaca O, Yilmaz T et al (2010) Experimental investigation of a novel desiccant cooling system. Energ Buildings 42:2049–2060
7. Bourdoukan P, Wurtz E, Joubert P et al (2008) Potential of solar heat pipe vacuum collectors in the desiccant cooling process: modeling and experimental results. Sol Energy 82:1209–1219
8. Enteria N, Mizutani K, Monma Y et al (2011) Experimental evaluation of the new solid heat pump system in Asia-Pacific climatic conditions. Appl Therm Eng 31:243–257
9. Cho WH, Kato S (2011) Outline of batch type desiccant air-conditioning system and humidification-heating performance. Part 1: Study on development of residential desiccant air-conditioning system and its performance evaluation. Archit Inst Jpn J Environ Eng 75:835–844
10. Finocchiaro P, Beccali M, Nocke B (2012) Advanced solar assisted desiccant and evaporative cooling system equipped with wet heat exchanger. Sol Energy 86:608–618
11. Bejan A (2006) Advanced engineering thermodynamics. Wiley, New Jersey
12. Hepbasli A (2008) A key review on exergetic analysis and assessment of renewable energy resources for a sustainable future. Renew Sust Energ Rev 12:593–661
13. Li H, Yang HX (2010) Energy and exergy analysis of multi-functional solar-assisted heat pump system. Int J Low-Carbon Technol 5:130–136
14. Rosen M (2001) The exergy of stratified thermal energy storages. Sol Energy 71:173–185
15. Kaushik SC, Siva Reddy V, Tyagi SK (2011) Energy and exergy analyses of thermal power plants: a review. Renew Sust Energ Rev 15:1857–1872
16. Fakheri A (2010) Second law analysis of heat exchangers. J Heat Transf 132:1–7
17. Caliskan H, Dincer I, Hepbasli A (2011) Exergetic and sustainability performance comparison of novel and conventional air cooling systems for building applications. Energ Buildings 43:1461–1472
18. Koroneos C, Nanaki E, Xydis G (2010) Solar air conditioning systems and their applicability—an exergy approach. Resour Conserv Recy 55:74–82
19. Marletta L (2010) Air conditioning systems from a 2nd law perspective. Entropy 12:859–877
20. Zhai H, Dai YJ, Wu JY et al (2009) Energy and exergy analyses on a novel hybrid solar heating, cooling and power generation system for remote areas. Appl Energ 86:1395–1404
21. Torio H, Anglotti A, Schmidth D (2009) Exergy analysis of renewable energy-based climatisation systems for buildings: a critical review. Energ Buildings 41:248–271

22. Kanoglu M, Carpinlioglu MO, Yildirim M (2004) Energy and exergy analyses of an experimental open-cycle desiccant cooling system. Appl Therm Eng 24:919–932
23. La D, Li Y, Dai YJ (2012) Development of a novel rotary desiccant cooling cycle with isothermal dehumidification and regenerative cooling using thermodynamic analysis method. Energy 44:778–791
24. Pons M, Kodama A (2000) Entropic analysis of adsorption open cycles for air conditioning. Part 1: first and second law analyses. Int J Energ Res 24:251–262
25. Hurdogan E, Buyukalaca O, Hepbasli A (2011) Exergetic modeling and experimental performance assessment of a novel desiccant cooling. Energ Buildings 43:1489–1498
26. Enteria N, Yoshino H, Mochida A (2013) First and second law analysis of the developed solar-desiccant cooling system. Energ Buildings 60:239–251
27. Lavan Z, Monnier JB, Worek WM (1982) Second law analysis of desiccant cooling systems. J Sol Energy Eng 104:229–236
28. Kodama A, Jin W, Goto M (2000) Entropic analysis of adsorption open cycles for air conditioning. Part 2: Interpretation of experimental data. Int J Energ Res 24:263–278
29. Shen CM, Worek WM (1996) The second-law analysis of a recirculation cycle desiccant cooling system: cosorption of water vapor and carbon dioxide. Atmos Environ 30:1429–1435
30. Enteria N, Yoshino H, Satake A (2010) Experimental heat and mass transfer of the separated and coupled rotating desiccant wheel and heat wheel. Exp Therm Fluid Sci 34:603–615
31. Rosen MA, Dincer I, Kanoglu M (2008) Role of exergy in increasing efficiency and sustainability and reducing environmental impact. Energ Policy 36:128–137
32. Dincer I, Rosen M (2013) Exergy: energy, environment and sustainable development. Elsevier, UK
33. Caliskan H, Hepbasli A, Dincer I et al (2011) Thermodynamic performance assessment of a novel air cooling cycle: Maisotsenko cycle. Int J Refrig 34:980–990
34. Kanoglu M, Bolatturk A, Altuntop N (2007) Effect of ambient conditions on the first and second law performance of an open desiccant cooling process. Renew Energ 32:931–946
35. Xiong ZQ, Dai YJ, Wang RZ (2010) Development of a novel two-stage liquid desiccant dehumidification system assisted by $CaCl_2$ solution using exergy analysis method. Appl Energ 87:1495–1504
36. Gebreslassie BH, Medrano M, Boer D (2010) Exergy analysis of multi-effect water-LiBr absorption systems: from half to triple effect. Renew Energ 35:1773–1782
37. Kaushik SC, Arora A (2009) Energy and exergy analysis of single effect and series flow double effect water-lithium bromide absorption refrigeration systems. Int J Refrig 32:1247–1258
38. Luo HL, Dai YJ, Wang RZ (2006) Experimental investigation of a solar adsorption chiller used for grain depot cooling. Appl Therm Eng 26:1218–1225
39. Askalany AA, Salem M, Ismael IM (2013) An overview on adsorption pairs for cooling. Renew Sust Energ Rev 19:565–572
40. Wang RZ, Ge TS, Chen CJ (2009) Solar sorption systems for residential applications: options and guidelines. Int J Refrig 32:638–660
41. Enteria N, Yoshino H, Mochida A et al (2015) Exergoeconomic evaluation of desiccant-evaporative air-conditioning system at different regeneration and reference temperatures. Int J Refrig 56:81–98
42. Enteria N, Yoshino Y, Satake A (2016) Exergoenvironmental evaluation of the desiccant air-conditioning system subjected to different regeneration temperatures. Int J Refrig Air-Cond. doi: http://dx.doi.org/10.1142/S2010132516500231